Chapter

Recent Advances of Copper-64 Based Radiopharmaceuticals in Nuclear Medicine

Nasim Vahidfar, Mohsen Bakhshi Kashi, Saeed Afshar, Peyman Sheikhzadeh, Saeed Farzanefar, Yalda Salehi, Ebrahim Delpasand, Eóin N. Molloy, Siroos Mirzaei, Hojjat Ahmadzadehfar and Elisabeth Eppard

Abstract

Copper radioisotopes including copper-60/61/62, and -64 exhibit a wide range of decay characteristics, making them appropriate choices for diagnostic/therapeutic (theranostic) applications in nuclear medicine. One notable feature of copper is the feasible coordination chemistry, which makes radiolabeling of a wide range of chemical structures including antibodies, proteins, peptides, and other biologically relevant small molecules possible. This chapter will summarize common radiopharmaceuticals of copper-64 and their radiation dosimetry in order to highlight recent improvements of positron emission tomography diagnostics.

Keywords: copper-64, radiopharmaceuticals, medical imaging, positron emission tomography, oncology

1. Introduction

Targeted nuclear imaging has significantly improved modern diagnostic methods and therapeutic procedures [1] by allowing for better imaging contrast, enhanced therapy effectivity, and reduction of radiation dose to the patients [2, 3]. Several classes of substances, including endogenous biomolecules, exogenous natural products, and synthetic molecules can be used practically as molecular probes for imaging or therapy [1]. Typically, molecular imaging is considered as a revolution in association with diagnosis and monitoring of disease [4]. Currently, positron emission tomography/computed tomography (PET/CT), alongside other diagnostic modalities, is well established, particularly given advances of PET/CT in terms of its superior resolution, sensitivity, and imaging quantification. These characteristics have made PET/CT a preferred method for molecular imaging [5–7]. In particular, copper radioisotopes have attracted much attention among PET radionuclides [8, 9]. Copper is an essential trace element in all living organisms [10–13]. The available radioisotopes of copper, including copper-60 (60Cu), copper-61 (61Cu), copper-62 (62Cu),

and copper-64 (64Cu), are appropriate for molecular imaging/or therapeutic applications (**Table 1**) [14].

With a wide range of half-lives extending from 9.7 min to 12.7 h, copper provides a series of radioisotopes suited for diagnostic or therapeutic applications in nuclear medicine [13, 15]. Copper coordination chemistry has the ability to form complex compounds with many ligands including antibodies, peptides, proteins, and other relevant small molecules [14, 16]. The long half-life of $^{64/67}$Cu allows for sufficient accumulation of radiolabeled compounds in targeted organs, specific and proper uptake and, as a result, considerably higher contrast and image quality [14]. Each of the above-mentioned copper-based radioisotopes has variably preferable properties based on given applications. For example, the shorter half-life and higher positron decay fraction of copper-60 and -62 make them ideal radionuclides for imaging evaluation of radiotracers with faster pharmacokinetic procedures such as radiolabeled small molecules. In contrast, the longer half-life of ^{64}Cu would be appropriate for radiolabeling of chemical structures, in order to formulate radiopharmaceuticals with slower pharmacokinetics, including radiolabeled peptides, nanoparticles, monoclonal antibodies (mAbs), antibodies, and higher molecular weight polypeptides [14]. While all copper radioisotopes are currently used in clinical applications, ^{64}Cu has shown the most promising results in both preclinical and clinical studies [16]. In particular, the longer half-life of ^{64}Cu (12.7 h) allows for the extension of the imaging period, which in turn compensates for lower sensitivity [9]. In a study assessing resolution, the "Derenzo" phantom application, demonstrated that PET imaging qualities with ^{64}Cu are accurately comparable to fluorine-18 (^{18}F) [17]. As ^{64}Cu-radiopharmaceuticals for the evaluation of human morbidities are currently undergoing significant developments [18], this chapter will focus on ^{64}Cu-radiopharmaceuticals that have been already approved for clinical trials or are close to being transferred to clinical settings (**Table 2**).

Radioisotope	Half-life ($T_{1/2}$)	Decay mode (abundance %)	Energy (keV)	Source	Application
^{60}Cu	23.7 min	β^+ (93)	2940,3920	Cyclotron	Imaging
		γ (7)	511-467-826-1332		
^{61}Cu	3.3 h	β^+ (60)	1220,1159	Cyclotron	Imaging
		γ (40)	511-283-589-656		
^{62}Cu	9.7 min	β^+ (98)	2925	Cyclotron	Imaging
		γ (2)	511	Generator	
^{64}Cu	12.7 h	β^+ (19)	657	Cyclotron	Imaging/ Therapy
		γ (43)	511-1346		
		β^- (38.4)	573		
^{67}Cu	2.58 d	β^- (100)	575	Cyclotron	Therapy

Table 1.
Physical characterization of copper radioisotopes [11]. β = Beta decay, γ = Gamma decay.

	Radiopharmaceuticals	Condition or disease	Phase	Last update posted
^{60}Cu	—	—	—	—
^{61}Cu	—	—	—	—
^{62}Cu	[^{62}Cu]Cu-ethylglyoxal bis (thiosemicarbazone)	Renal failure	2	April, 2017 (Terminated)
^{64}Cu	[^{64}Cu]Cu-ATSM	Rectal cancer	2	May, 2021
		Cervical cancer	2	February, 2021
		NSCLC	N/A	July, 2013
	[^{64}Cu]Cu-DOTA-TATE	Neuroendocrine tumors	3	July, 2019 (Approved for marketing)
	[^{64}Cu]Cu-DOTA-alendronate	Breast carcinoma	Early 1	November, 2021
	[^{64}Cu] Cu-DOTA-trastuzumab	Gastric cancer	N/A	March, 2021
		Breast cancer	N/A	January, 2021
	[^{64}Cu]Cu-Rituximab	Non-Hodgkin's lymphoma	N/A	October, 2016
	[^{64}Cu]Cu-DOTA-ECL1i	Head and neck cancer	1	December, 2021
	[^{64}Cu]Cu-LLP2A	Multiple myeloma	Early 1	August, 2021
	[^{64}Cu]Cu-SARTATE	Neuroendocrine tumors	2	May, 2021
	[^{64}Cu]Cu-SAR-bisPSMA	Prostatic neoplasms	1	August, 2021
	[^{64}Cu]Cu-DOTA-TLX592	Metastatic prostate cancer	Early 1	August, 2021
	[^{64}Cu] Cu-DOTA-pembrolizumab	Hematopoietic and lymphoid cell neoplasm	1	November, 2021
	[^{64}Cu]Cu-Macrin			
	[^{64}Cu]Cu-NOTA-PSMAi-PEG-Cy5.5-C′ dots	Sarcoid	1	September, 2021
	[^{64}Cu]Cu-FBP8	Prostate cancer	1	September, 2021
		Pulmonary embolism	1	July, 2019

Table 2.
^{64}Cu radiopharmaceuticals list entered in clinical trials.

1.1 ^{64}Cu radiopharmaceuticals and their role in clinical studies

As it described above, ^{64}Cu is a promising radionuclide that can be incorporated into many bio-conjugated chemical structures to further develop diagnostic and therapeutic agents with specific oncological indications [19]. The intermediate half-life of copper-64 (12.7 h) and its' short positron range (comparable to fluorine-18) allow ^{64}Cu to create high-resolution PET tracers [20, 21]. Hypoxia imaging agents based on bis(thiosemicarbazone) complexes radiolabeled with ^{64}Cu have been used successfully for PET imaging of various types of tumors [22–24], blood flow [25], disease related to metabolism alterations [26–29], and cell tracking [30]. Free [^{64}Cu]$CuCl_2$ can also been used as a valuable radiopharmaceutical for quantifying physiological biodistribution of Cu in associated disorders including Wilson's and Menkes diseases

in preclinical studies [29, 31], Alzheimer's disease [32, 33], and cancer PET imaging (e.g., prostate cancer) [34]. Also, preclinical studies have shown the diagnostic efficiency of [^{64}Cu]$CuCl_2$ in a glioblastoma xenograft model [35]. Suitable visualization of the tumor by [^{64}Cu]$CuCl_2$ can provide a theory that supports the non-dependency of ^{64}Cu complexes on ligands for tumor accumulations [35]. The following passages will discuss notable applications of ^{64}Cu radiopharmaceuticals in accomplished clinical trials with the aim of clarifying new PET tracers' roles in nuclear medicine.

1.2 Imaging tumor hypoxia

In circumstances under which cells are deprived of oxygen, hypoxia will occur and resistance to radiotherapy or chemotherapy and risk of invasion and metastases increases [11, 36, 37]. Hypoxia is a common condition in 50–60% of locally advanced solid tumors [11]. In addition to variable levels in different tumors, heterogeneity in a particular tumor tissue also can affect the reliable estimation of hypoxia [38]. Given a specific physiological state in hypoxia cells, they can be diagnosed with medical imaging modalities [39]. As a result, there are various PET tracers, which specifically detect hypoxia in humans [40–42]. In a series of *ex-vivo* studies, Fujibayashi et al. initially identified the critical role of the lipophilic radioactive copper (II) complex of the N_2S_2 ligand termed [^{62}Cu]Cu-ATSM, specifically in relation to selective accumulation in hypoxia cells [43, 44]. Later, *in-vivo* studies demonstrated further that copper radiolabeled ATSMs have high specificity and selectivity as tracers for the detection of tumor hypoxia [45–49]. Despite the fact that the exact localization mechanism of Cu-ATSM is still not fully understood, theoretical evaluations suggest that Cu-ATSM can passively diffuse through cell membranes due to its high permeability. Moreover, due to the low redox potential of the tracer, it can be trapped constantly following the reduction process in hypoxic cells [14]. This reduction can only occur in hypoxic cells given that the abnormally reduced state of their mitochondria is not common in normoxic cells [43].

In a comparison study by Lewis et al., [^{64}Cu]Cu-ATSM, [^{64}Cu]Cu-PTSM, and [^{18}F]F-MISO were identified as the most promising tumor hypoxia radiopharmaceuticals while also showing that the former ([^{64}Cu]Cu-ATSM), exhibits heterogeneous oxygen concentration-dependent accumulation in different cells compared to the more stable uptake of the [^{64}Cu]Cu-PTSM and [^{18}F]F-MISO [50]. Also, [^{64}Cu]Cu-ATSM presented faster clearance from normal tissues compared to the other tumor hypoxia tracers [51]. All in all, previous data show that PET/CT utilizing [^{64}Cu]Cu-ATSM is a reliable and non-invasive imaging method that can accurately map hypoxic areas [52, 53]. In a clinical study of 10 cervical cancer patients, results showed that the signal-to-noise ratio was superior for [^{64}Cu]Cu-ATSM was superior to [^{60}Cu]Cu-ATSM. Consequently, [^{64}Cu]Cu-ATSM has been proposed as a safe radiopharmaceutical that can be used to achieve high-quality imaging in tumor hypoxia cases [54]. Moreover, these data also showed that imaging reproducibility is feasible for up to 9 days. Accordingly, the authors concluded that [^{64}Cu]Cu-ATSM is an ideal radiotracer for chronic tumor hypoxia rather than as an acute condition [55].

Furthermore, in a case report on a glioblastoma multiforme (GBM) patient, the authors observed accumulation of [^{64}Cu]Cu-ATSM from early acquisition to late acquisition in hypoxia sites as well as high correlation between ^{64}Cu-ATSM PET/CT results and HIF-1α expression as a hypoxia marker [56]. Feasibility of ^{64}Cu-ATSM PET/CT in both cervical cancer and lung cancer has also been previously demonstrated [57–59], while in a comparative clinical study in 11 patients with head and

neck cancer treated with chemoradiotherapy, the efficacy of [^{64}Cu]Cu-ATSM and [^{18}F]FDG was evaluated [60]. According to the findings of [^{64}Cu]Cu-ATSM in seven patients, nodal metastases were detected and 22 cancer foci were identified in total calculated amounts for sensitivity and specificity of [^{64}Cu]Cu-ATSM based on evaluated SUVmax were 100 and 50% and the same estimation considering the volume were 100 and 33%, respectively [60]. In conventional theories accumulation mechanism of [^{64}Cu]Cu-ATSM was interpreted based on ^{64}Cu(II) oxidation state [43, 61]. It was proposed that ^{64}Cu(II) be reduced to ^{64}Cu(I) by NADH/NADPH under the hypoxia circumstances. According to the lower stability of ^{64}Cu(I) compared to ^{64}Cu(II) dissociation of the [^{64}Cu]Cu-ATSM results in H2-ATSM and free Cu ions [50]. However, the exact reduction process is under debate until now. Colombié et al. reported that the functional mechanism of [^{64}Cu(II)]-Cu-ATSM is related to redox potential and formation of reactive oxygen species which can appear under the hypoxia cellular condition [53]. Further studies suggest that the accumulation of [^{64}Cu(II)]-Cu-ATSM is not mediated depending on the oxygen pressure of the tumors [62]. In sum, these results show a comparable efficacy between [^{64}Cu] Cu-ATSM and [^{18}F]FDG PET/CT in the estimation of biological tumor volume (BTV), while clarifying that [^{64}Cu]Cu-ATSM has higher sensitivity and lower specificity in predicting neoadjuvant chemoradiotherapy responses [60].

1.3 Tumor targeting by radiolabeled antibodies

1.3.1 [^{64}Cu]Cu-trastuzumab

Epidermal growth factor receptor (ErbB) is composed of four closely related members including ErbB-1 (HER1 or epidermal growth factor receptor, EGFR), ErbB-2 (HER2), ErbB-3 (HER3), and ErbB-4 (HER4). HER1, HER3, and HER4 bind to approximately a dozen of different ligands while HER2 has no specific ligand [63, 64]. Previously, it has been demonstrated that HER2 is activated through dimerization with other HER derivatives. This complex will subsequently activate intracellular signaling pathways of MAPK (mitogen-activated protein kinase) and PI3K (phosphoinositide 3-kinase) [65]. These pathways are responsible for tumor growth, invasion, migration, and survival while gene coding associated with breast cancer can amplify 15–20% of them [66, 67]. Gene amplification or protein overexpression are notable criteria for the candidacy of breast cancer patients from primary to metastatic stages for HER2-directed therapy [63]. Trastuzumab is confirmed as the first-line of a therapeutic plan for HER2-positive in advanced breast cancer [68]. Trastuzumab is a humanized antibody that binds to the extracellular domain of HER2 and inhibits the proliferation progress [69]. It was demonstrated as a remarkable point that [^{64}Cu]Cu-trastuzumab can be used for pretreatment assessment of breast cancer. Since measurements of [^{64}Cu]Cu-trastuzumab uptake in lesions is a very promising criterion of patient selection for treatment procedures [63]. In a clinical trial performed of five HER2-positive breast cancer patients, results indicated that [^{64}Cu]Cu-trastuzumab PET/CT scan is a safe and feasible for non-invasive and serial detection of HER2 status in metastatic brain tumors [70]. Based on clinical trials, [^{64}Cu]Cu-trastuzumab can be efficient for the diagnosis of metastases related to other malignancies [71]. For instance, radiolabeled trastuzumab can be mentioned as a standard tracer for HER2-positive gastric or gastro-esophageal junction cancer patients [72]. Moreover, a recent clinical trial compared [^{64}Cu]Cu-NOTA-trastuzumab in a HER2-positive primary gastric cancer patient with liver metastases,

to [^{18}F]FDG [73] with results showing comparable outcomes. Specifically, six liver metastases >1 cm were identified by both detection radiopharmaceuticals. Two metastases <0.5 cm were detected only with [^{18}F]FDG and were not easily identified with [^{64}Cu]Cu-NOTA-trastuzumab [73]. However, SUVmax of [^{64}Cu]Cu-NOTA-trastuzumab in the primary lesion was estimated 28.6 ± 0.50 versus 13.5 ± 0.30 for [^{18}F]FDG [73]. Based on comparable clinical results between [^{18}F]FDG and [^{64}Cu]Cu-trastuzumab attained by these data, it can be argued that further clinical evaluations of [^{64}Cu]Cu-trastuzumab are needed.

1.3.2 [^{64}Cu]Cu-rituximab

Rituximab (RTX) is a chimeric human/murine mAb that targets CD20 positive B-cell malignancies and has been used for immunotherapy of patients with non-Hodgkin's lymphoma (NHL) [74, 75]. Radiolabeling of RTX with (β^-/β^+) emitters could augment the antibodies' theranostic activity. In this regard, ^{64}Cu-labeled RTX ([^{64}Cu]Cu-DOTA-rituximab) as a PET imaging agent could be used to track the progress of NHL treatment [75]. The ongoing pre-clinical trial using [^{64}Cu]Cu-DOTA-rituximab PET/CT was established to determine the tracers' pharmacokinetics, biodistribution, stability, uptake, and radiation dosimetry in CD20-positive B-cell NHL patients compared to the [^{18}F]FDG PET/CT [76]. Following this study, Natarjan et al. reported validated production of [^{64}Cu]Cu-rituximab under good manufacturing practices (GMP) in order to clinical indication for the diagnosis of CD20 positive B-cell non-Hodgkin lymphoma [75]. Finally based on strong evidences efficacy of [^{64}Cu]Cu-rituximab in detecting of B-cells in a murine model of MS was confirmed [77]. This achievement can be very hopeful in detection or even early diagnosis of MS in patients who respond to anti-B-cell therapies.

1.4 Tumor targeting by radiolabeled somatostatin derivatives: [^{64}Cu]Cu-DOTA-TATE, and [^{64}Cu]Cu-DOTA-TOC

Somatostatin receptors (SSTR) have been reported as qualified targets for the evaluation of neuroendocrine tumors (NETs) [78]. After [^{68}Ga]Ga-DOTA-TATE, which was introduced as a gold standard for diagnosis purposes of NETs, it was hypothesized that ^{64}Cu would be superior for radiolabeling of somatostatin derivatives [78]. The physical properties of ^{64}Cu compared to ^{68}Ga, including longer half-life (12.7 h versus 67.7 min for ^{68}Ga), and shorter positron range (1 mm versus 4 mm), makes ^{64}Cu more accessible radionuclide with higher spatial resolution for clinical studies [79]. Various comparative studies have been performed to clarify the emphasis of radiolabeled somatostatin derivatives with ^{64}Cu. In a clinical trial study of 59 NET patients carried out by Johnbeck and colleagues, the authors compared diagnostic results derived from [^{68}Ga]Ga-DOTA-TOC and [^{64}Cu]Cu-DOTA-TATE PET/CT radiopharmaceuticals [78]. Results showed that 701 lesions were concordantly recognized with both radiopharmaceuticals. However, in detection of 68 lesions, there were no correlation between the [^{68}Ga]Ga-DOTA-TOC and [^{64}Cu]Cu-DOTA-TATE. Forty-two lesions were detected only by [^{64}Cu]Cu-DOTA-TATE, of which 33 were found to be true positives. Moreover, only 26 lesions were found with [^{68}Ga]Ga-DOTA-TOC, of which seven were true positive [78]. These results demonstrated that [^{64}Cu]Cu-DOTA-TATE exhibits higher specificity and sensitivity compared to [^{68}Ga]Ga-DOTA-TOC [78].

Further studies have confirmed that [^{64}Cu]Cu-DOTA-TATE's role as a safe imaging protocol in providing of accurate and high-quality images for diagnosis, treatment, and follow-up of NETs [80–83]. In accomplished comparative clinical studies for [^{64}Cu]Cu-DOTA-TATE, [^{99m}Tc]Tc-HYNIC-octreotide, and [^{111}In]In-DTPA-OC, superiority of [^{64}Cu]Cu-DOTA-TATE in the diagnosis of NETs was demonstrated [82, 84]. [^{64}Cu]Cu-DOTA-TATE is the most appropriate choice for the diagnosis of NETs due to robust manufacturing with no need for regional generators, and a longer half-life allowing a wide geographical range for commercial distribution. This drug was approved in September 2020 by FDA and is now commercially available in the USA. **Figures 1**–**3** display detection rate of [^{64}Cu]Cu-DOTA-TATE in NETs. In a clinical trial [^{64}Cu]Cu-MeCOSar-Tyr^3-octreotate ([^{64}Cu]Cu-SARTATE) was applied in [^{68}Ga]Ga-DOTA-TATE positive NET patients [85]. A significant advantage of this radiopharmaceutical compared to [^{68}Ga]Ga-DOTA-TATE is the higher stability of sarcophagine (Sar) linker versus DOTA. The concluded results showed comparable diagnosis visualization in 9 of 10 patients in 1 h imaging. In one patient a liver lesion was missed by [^{64}Cu]Cu-SARTATE. However, the imaging obtained in 24 h, demonstrated the diagnostic superiority of [^{64}Cu]Cu-SARTATE compared to [^{68}Ga]Ga-DOTA-TATE [85].

Several somatostatins analogs radiolabeled with SPECT and PET radionuclides have been evaluated in clinical trials to ascertain a possible gold standard for the diagnosis and treatment of NETs [86]. To date, 68Ga radiolabeled somatostatin derivatives including DOTA-TOC, DOTA-TATE, and DOTA-NOC (**Figure 4**) have shown promising results as diagnostic radiopharmaceuticals for NETs [78]. Recently, it was also demonstrated that 64Cu radiolabeled somatostatin analogs have advantages compared to former radiopharmaceuticals, some of which are discussed previously.

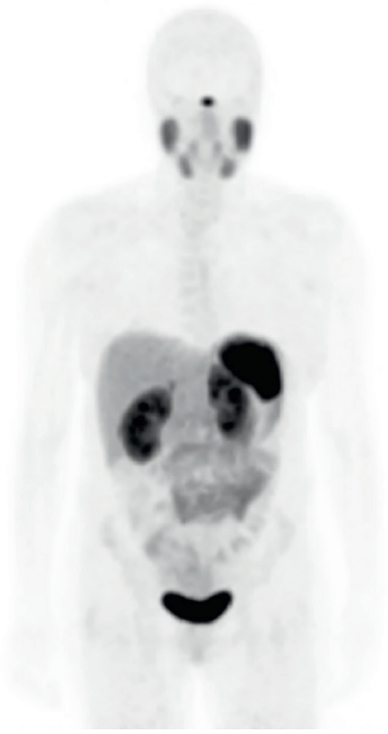

Figure 1.
Physiologic uptake is seen in the pituitary, salivary, and lacrimal glands, liver, spleen, GI tract, adrenals, kidneys, and urinary bladder. Mild & diffuse bone marrow uptake or focal activity in the pancreas might occur as normal physiologic variants (e.g., uncinate process of the pancreas). (Courtesy of Courtesy Ebrahim Delpassand, MD RadioMedix, Inc. Houston, TX, USA).

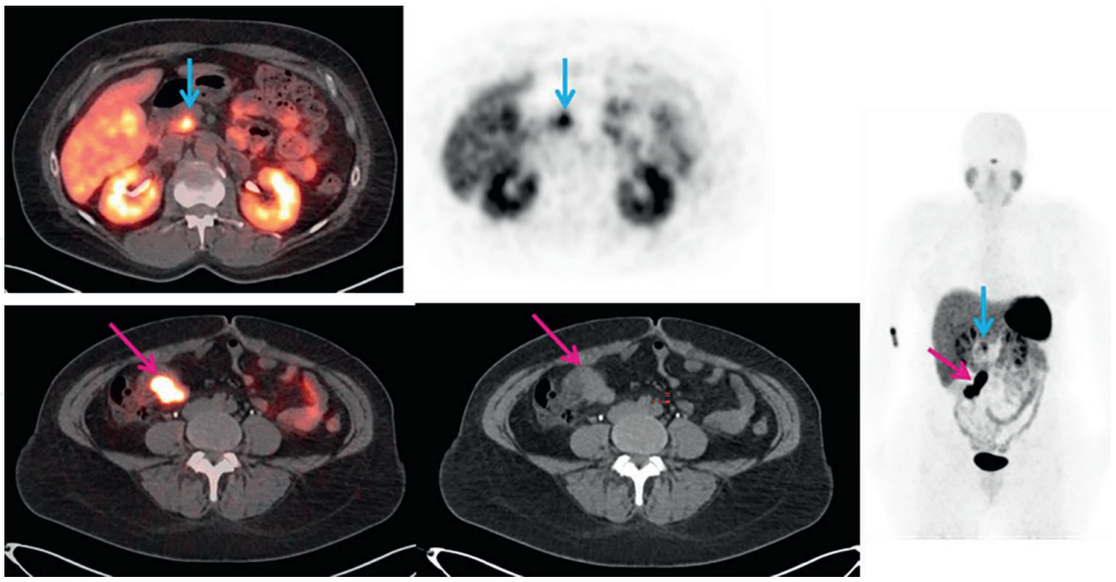

Figure 2.
53-year-old female with newly diagnosed neuroendocrine tumor in the terminal ileum. The red arrow points to the primary tumor. The blue arrow points to the uncinate process uptake, which is a normal physiological variant. (Courtesy Ebrahim Delpassand, MD, RadioMedix, Inc. Houston, TX, USA).

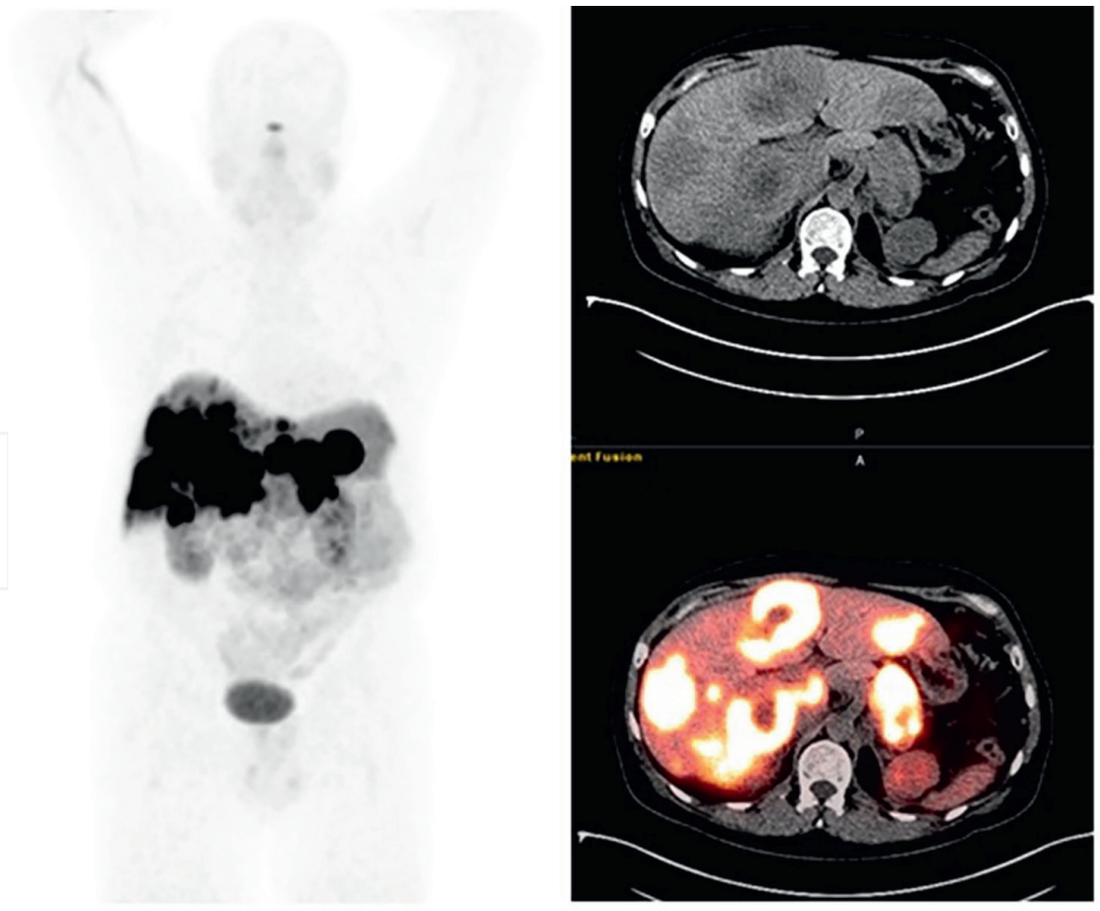

Figure 3.
49-year-old male with pancreatic neuroendocrine tumor. On the fused [^{64}Cu]Cu-DOTA-TATE PET/CT images a [^{64}Cu]Cu-DOTA-TATE avid lesion is noted in the pancreatic tail. Also, multiple hypodense [^{64}Cu]Cu-DOTA-TATE avid lesions are noted in both liver lobes suggesting metastatic involvement. (Courtesy Courtesy Ebrahim Delpassand, MD RadioMedix, Inc. Houston, TX, USA).

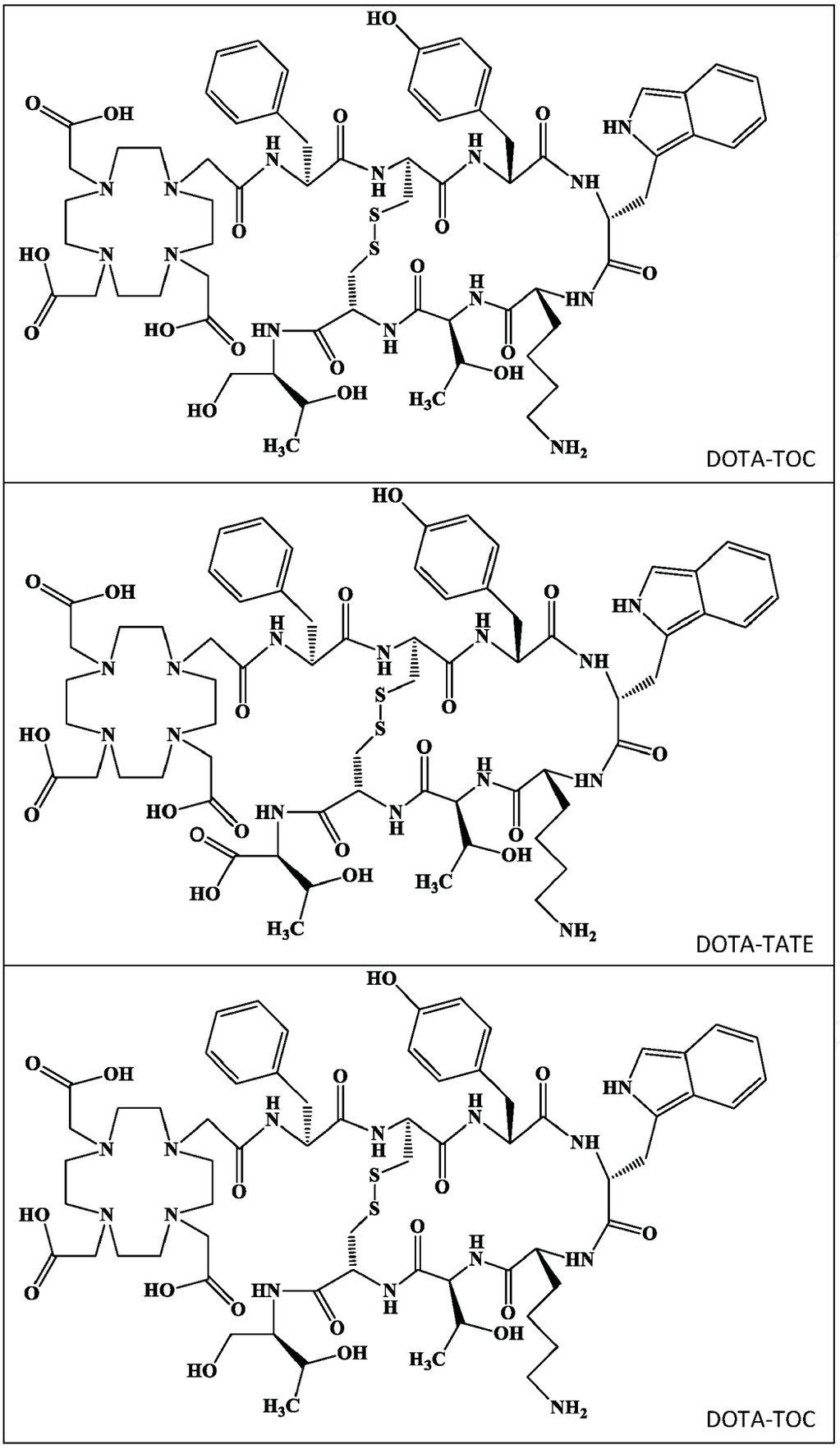

Figure 4.
Chemical structures of DOTA-TOC (top), DOTA-TATE (middle), and DOTA-NOC (bottom).

In a retrospective study, 33 patients with NETs who had surgically removed primary lesions, underwent [^{64}Cu]Cu-DOTA-TOC PET/CT scan [87]. Five patients exhibited no detectable pathological lesion in PET/CT scan, while eight showed enhanced uptake at the skull base, and 20 presented at least one pathological lesion [87]. Based on this clinical trial, it was concluded that [64Cu]Cu-DOTA-TOC PET/CT scan can differentiate NET lesions with a feature of high target-to-background contrast [87]. Interestingly, these findings also correlated with [177Lu]Lu-DOTA-TATE results obtained from a follow-up assessment in another patient's group [87]. Further studies on larger populations are needed to identify the most appropriate somatostatin derivative for NETs diagnosis in radiolabeling with 64Cu. As an example, (**Figure 5**) displays the detection rate of [^{64}Cu]Cu-DOTA-TOC in NET of the bladder.

1.5 Tumor targeting by radiolabeled PSMA ligands

1.5.1 [^{64}Cu]Cu-PSMA-617

Previous studies have been demonstrated that prostate-specific membrane antigen (PSMA) is over expressed in prostate cancer (PCa) [88], suggesting that PSMA can be used as a potent tumor marker for PCa, as well as a vital target for imaging and therapy [88]. Among the recognized radiolabeled PSMA inhibitors, it has been shown that [^{68}Ga]Ga-PSMA-11 is highly effective as a PET tracer for the detection of PCa [88]. Furthermore, PSMA can also be radiolabeled with ^{64}Cu, offering a longer half-life and higher spatial resolution [89]. In a comparative clinical trial, the biodistribution of [^{64}Cu]Cu-PSMA-617 and [^{68}Ga]Ga-PSMA-11 were assessed in PCa patients [89]. Diagnostic results showed that both radiopharmaceuticals show similar biodistribution, except the excretion route, in which [^{64}Cu]Cu-PSMA-617 excreting takes place through the gastrointestinal tract rather than the renal excretion of [^{68}Ga]Ga-PSMA-11 [89]. The low metabolic rate of PCa cells leads to negligible uptake of [^{18}F]FDG in PCa. [^{18}F]FDG accumulates based on glucose consumption and as a consequence of the mentioned fact unacceptable specificity of [^{18}F]FDG for the detection of PCa is raised [90–92]. However, it has also been demonstrated that [^{18}F]FDG is useful for selected PCa patients with hormone-resistant poorly differentiated cell types [93–95].

Choline is an essential precursor for phospholipid synthesis of membranes in normal cells and based on the proliferation rate, uptake of choline increases mainly in cancerous cells [96, 97]. [^{18}F]F-choline ([^{18}F]FCH) PET/CT has been used for the detection of PCa widely during the last decade and optimistic results have been achieved [90]. It assessed that [^{18}F]FCH PET/CT is useful for detection of local and distant nodal recurrence and bone metastases [90, 98–100]. In another cohort study, the efficacy of [^{64}Cu]Cu-PSMA-617 and [^{18}F]FCH PET/CT was compared [101]. This study, conducted on 43 patients, assessed restaging after biochemical recurrence [101]. In terms of detection rate, results indicated no statistically significant differences. However, [^{64}Cu]Cu-PSMA-617 showed better performance with overall positivity at 74.4% compared to 44.2% for [^{18}F]FCH [101]. This retrospective study demonstrated that [^{64}Cu]Cu-PSMA-617 is promising in the prediction and assessment of recurrent sites relative to other PET tracers [101].

In another clinical trial performed by Grubmuller et al., it was shown that [^{64}Cu]Cu-PSMA-617 has high potential as a PET tracer in detection of recurrent cases or progressive local lesions in primary staging of PCa patients [102]. In comparison to [^{68}Ga]

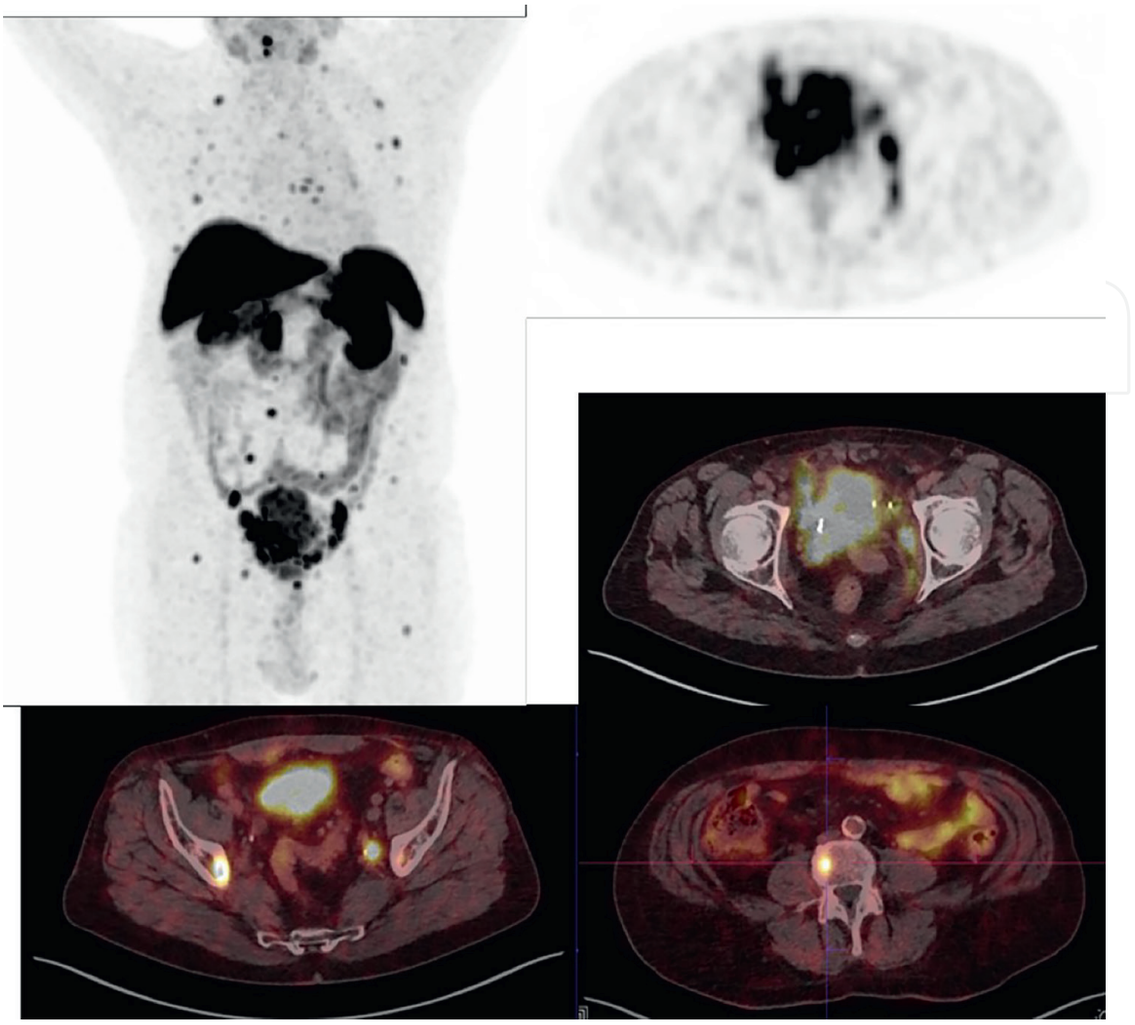

Figure 5.
68-year-old male patient with a neuroendocrine tumor of the bladder (G3) with multiple pelvic LN and bone metastases. Additionally, we see the primary tumor in the bladder with infiltration into the surrounding tissue. [^{64}Cu]Cu-DOTA-TOC (179 MBq) PET/CT. (Courtesy of Clinic Ottakring, Institute of Nuclear Medicine with PET-Center, Vienna, Austria).

Ga-PSMA-11, higher image quality resulting from higher image contrast and superior uptake for [^{64}Cu]Cu-PSMA-617 was shown, suggests the latter as an appropriate radiopharmaceutical compared to conventional PCa radiotracers [102]. Subsequently, [^{64}Cu]$CuCl_2$ has also been reported as an applicable diagnostic tracer for PCa [34, 103]. Cu is an essential requirement for normal cells in signaling transduction pathways of proliferation processes [104]. So increased uptake of Cu in aggressive uncontrolled cancerous prostate cells with a high proliferation rate would be inevitable [103]. In a previous study 50 patients with biochemical relapse PCa after surgery or external beam radiation therapy went through [^{64}Cu]$CuCl_2$ and [^{18}F]F-choline PET/CT scans [34], results indicated that biodistribution of [^{64}Cu]$CuCl_2$ is more appropriate for exploring the prostate and pelvic bed. Finally, it was shown that in patients with relapsed PCa and low levels of PSA, [^{64}Cu]$CuCl_2$ has a higher detection rate compared to [^{18}F]F-choline [34]. In sum, it can be argued that [^{64}Cu]$CuCl_2$ is a suitable tracer for the primary staging of PCa and regional lymph nodes [103]. However, based on high diagnostic accuracy, [^{64}Cu]Cu-PSMA-617 has been suggested in both primary staging in patients with progressive local disease and recurrent cases [102, 105, 106].

Pharmaceutical	Dose (MBq)	Average effective dose (mSv/MBq)	Study type	Organs with highest absorbed dose (mGy/MBq)	Ref.
[^{64}Cu]Cu-DOTA-trastuzumab	115–136	0.036 ± 0.009 (mean: 4.5 mSv)	Patient	Heart: 0.340	[71]
				Liver: 0.237	
				Spleen: 0.142	
[^{64}Cu]Cu-NOTA-trastuzumab	3.7	—	Animal/ Monte Carlo simulation	Heart: 0.048	[107]
				Liver: 0.079	
				Spleen: 0.047	
[^{64}Cu] Cu-PSMA-617	18.7* 119–160#	0.0292	Animal/ patient	Gallbladder wall: 2.04	[108]
				Liver: 0.014	
				Kidney: 0.009	
[^{64}Cu] Cu-DOTA-TATE	193–232	0.0315	Patient	Pituitary gland: 0.19	[109]
				Liver: 0.16	
				Kidneys: 0.14	
[^{64}Cu]Cu-DOTA-pembrolizumab	7.4	0.004	Animal[a]	Liver: 0.032	[110]
				Red marrow: 0.018	
				Lungs: 0.010	
[^{64}Cu]Cu-TETA-OC	107–130#	0.013	Animal/ patient	Bladder wall: 0.25	[111]
				Liver: 0.092	
				Kidneys: 0.078	
[^{64}Cu] Cu-DOTA-AE105	197–213	0.0276	Human	Liver: 0.175	[112]
				Kidney: 0.0562	
[^{64}Cu]Cu-DOTA-alendronate	37–74	0.0418	Animal[b]	LLI wall: 0.159	[113]
				ULI wall: 0.113	
				Kidneys: 0.108	
[^{64}Cu]Cu-Cl_2	4.0 MBq/kg	0.051 (m)	Human	Liver: 0.310 (m)	[114]
				Liver: 0.421 (f)	
		0.061 (f)		LLI wall: 0.153 (m)	
				LLI wall: 0.161 (f)	
[$^{60/61/62/64}$Cu] Cu-ATSM	480[1]	0.011[1]	Animal/ patients[c]	Liver: 0.064[1]	[115]
		0.029[2]		Liver: 0.275[2]	
		0.003[3]		Liver: 0.017[3]	
		0.036[4]		Liver: 0.390[4]	
[^{64}Cu] Cu-SARTATE	192	0.0454	Human	Spleen: 0.361	[85]
				Kidneys: 0.202	
				Adernals: 0.169	

Pharmaceutical	Dose (MBq)	Average effective dose (mSv/MBq)	Study type	Organs with highest absorbed dose (mGy/MBq)	Ref.
[^{64}Cu]Cu-DOTA-Rituximab	7.4	0.024	Animal[b]	Spleen: 0.098 Liver: 0.051 Osteogenic cells: 0.042	[76]

LLI wall: lower large intestine wall.
ULI wall: upper large intestine wall.
m: men.
f: women.
**mice.*
#patient.
[1]copper-60.
[2]copper-61.
[3]copper-62.
[4]copper-64.
[a]based on ex-vivo biodistribution and PET/CT images.
[b]estimation for humans.
[c]dose estimation for human based on copper-60.

Table 3.
Injected dose level, estimated absorbed doses, and organs at risk in [^{64}Cu]Cu-radiopharmaceuticals.

2. Pre-clinical and clinical dosimetry results of ^{64}Cu-radiopharmaceuticals

Table 3 shows the results of the injected dose level and the estimated absorbed doses and organs at risk in ^{64}Cu radiopharmaceuticals. Based on previous studies on ^{64}Cu-radiopharmaceuticals, injected dose levels for patients were between 105 and 192 MBq which is about half of [^{18}F]FDG dose and provided acceptable image quality. The calculated effective absorbed dose for the total body with ^{64}Cu-radiopharmaceuticals in human studies or in animal studies indicated a range of 0.01–0.06 mSv/MBq. In the case of radiation potential hazards, these ranges are within an acceptable level and lower than other similar radiopharmaceuticals.

3. Conclusion

The number of developing ^{64}Cu labeled radiopharmaceuticals is growing. The most considerable characteristics of ^{64}Cu include a longer half-life and superior image quality, resulting in high image contrasts, robust centralized manufacturing, and wider geographical range of distribution and ease of use by the end user. These characteristics have led to the introduction of novel and promising ^{64}Cu radiopharmaceuticals in both pre-clinical and clinical trials. [^{64}Cu]Cu- DOTATATE (Detectnet™) is the first ^{64}Cu labeled radiopharmaceutical approved by the FDA and is commercially available in the USA. ^{64}Cu/^{67}Cu pair has great and true theranostic applications. Impressive numbers of clinical trials using ^{64}Cu labeled compounds suggest that the menu of approved radiopharmaceuticals in this field will increase in the near future.

Abbreviations

ATSM:	diacetyl-bis(N4-methylthiosemicarbazone)
BTV:	biological tumor volume
CD20:	cluster of differentiate 20
CT:	computed tomography
Cu:	copper
DOTA:	2,2′,2”,2”'-(1,4,7,10-tetraazacyclododecane-1,4,7,10-tetrayl)tetraacetic acid
FCH:	fluorocholine
FDG:	fludeoxyglucose
FDA:	food and drug administration
Ga:	gallium
GBM:	glioblastoma multiform
GI:	gastro intestinal
HER:	human epidermal growth factor receptor
MAb:	monoclonal antibody
MAPK:	mitogen-activated protein kinases
MBq:	mega becquerel
MISO:	misonidazole
NADH:	nicotinamide adenine dinucleotide (NAD) + hydrogen (H)
NADPH:	nicotinamide adenine dinucleotide phosphate
NET:	neuroendocrine tumors
NHL:	non-Hodgkin lymphoma
NOC:	[Nal3]-octreotide
NOTA:	2,2′-(7-(2-((2,5-dioxopyrrolidin-1-yl)oxy)-2-oxoethyl)-1,4,7-triazonane-1,4-diyl)diacetic acid
PCa:	prostate cancer
PET:	positron emission tomography
PTSM:	pyruvaldehyde-bis(N4-methylthiosemicarbazone)
PSA:	prostate specific antigen
PSMA:	prostate specific membrane antigen
RTX:	Rituximab
SAR:	sarcophagine
SPECT:	single-photon emission computed tomography
SSTR:	somatostatin receptor
TATE:	[Tyr3]-octreotate
TOC:	[Tyr3]-octreotide

DOI: http://dx.doi.org/10.5772/intechopen.1003993

Author details

Nasim Vahidfar[1], Mohsen Bakhshi Kashi[1], Saeed Afshar[1], Peyman Sheikhzadeh[1], Saeed Farzanefar[1], Yalda Salehi[1], Ebrahim Delpasand[2,3], Eóin N. Molloy[4,5], Siroos Mirzaei[6], Hojjat Ahmadzadehfar[7] and Elisabeth Eppard[4]*

1 Department of Nuclear Medicine, Vali-Asr Hospital, Tehran University of Medical Sciences, Tehran, Iran

2 RadioMedix, Inc., Houston, TX, USA

3 Excel Diagnostics and Nuclear Oncology Center, Houston, TX, USA

4 University Clinic for Radiology and Nuclear Medicine, Faculty of Medicine, Otto von Guericke University (OvGU), Magdeburg, Germany

5 Multimodal Neuroimaging Lab, German Centre for Neurodegenerative Diseases, Magdeburg, Germany

6 Clinic Ottakring, Institute of Nuclear Medicine with PET-Center, Vienna, Austria

7 Department of Nuclear Medicine, Klinikum Westfalen, Dortmund, Germany

*Address all correspondence to: elisabeth.eppard@med.ovgu.de

References

[1] Boschi A, Martini P, Janevik-Ivanovska E, Duatti A. The emerging role of copper-64 radiopharmaceuticals as cancer theranostics. Drug Discovery Today. 2018;**23**:1489-1501

[2] Oyen W, Bodei L, Giammarile F, Maecke H, Tennvall J, Luster M, et al. Targeted therapy in nuclear medicine—Current status and future prospects. Annals of Oncology. 2007;**18**:1782-1792

[3] Stéen EJL, Edem PE, Nørregaard K, Jørgensen JT, Shalgunov V, Kjaer A, et al. Pretargeting in nuclear imaging and radionuclide therapy: Improving efficacy of theranostics and nanomedicines. Biomaterials. 2018;**179**:209-245

[4] Ma MT, Donnelly PS. Peptide targeted copper-64 radiopharmaceuticals. Current Topics in Medicinal Chemistry. 2011;**11**:500-520

[5] Jones T, Townsend DW. History and future technical innovation in positron emission tomography. Journal of Medical Imaging. 2017;**4**:011013

[6] Duclos V, Iep A, Gomez L, Goldfarb L, Besson FL. PET molecular imaging: A holistic review of current practice and emerging perspectives for diagnosis, therapeutic evaluation and prognosis in clinical oncology. International Journal of Molecular Sciences. 2021;**22**:4159

[7] Lebech A-M, Gaardsting A, Loft A, Graff J, Markova E, Bertelsen AK, et al. Whole-body 18F-FDG PET/CT is superior to CT as first-line diagnostic imaging in patients referred with serious nonspecific symptoms or signs of cancer: A randomized prospective study of 200 patients. Journal of Nuclear Medicine. 2017;**58**:1058-1064

[8] International BR. Retracted: The copper radioisotopes: A systematic review with special interest to 64Cu. BioMed Research International. 2018;**2018**:1. Article ID 3860745. DOI: 10.1155/2018/3860745

[9] Williams HA, Robinson S, Julyan P, Zweit J, Hastings D. A comparison of PET imaging characteristics of various copper radioisotopes. European Journal of Nuclear Medicine and Molecular Imaging. 2005;**32**:1473-1480

[10] Kodama H, Fujisawa C. Copper metabolism and inherited coppertransport disorders: Molecular mechanisms, screening, and treatment. Metallomics. 2009;**1**:42-52

[11] Hao G, Singh AN, Oz OK, Sun X. Recent advances in copper radiopharmaceuticals. Current Radiopharmaceuticals. 2011;**4**:109-121

[12] Tapiero H, Townsend DÁ, Tew K. Trace elements in human physiology and pathology. Copper. Biomedicine & Pharmacotherapy. 2003;**57**:386-398

[13] Gutfilen B, Souza SA, Valentini G. Copper-64: A real theranostic agent. Drug Design, Development and Therapy. 2018;**12**:3235

[14] Zhou Y, Li J, Xu X, Zhao M, Zhang B, Deng S, et al. 64Cu-based radiopharmaceuticals in molecular imaging. Technology in Cancer Research & Treatment. 2019;**18**:1533033819830758

[15] Bhargava KK, Gupta RK, Nichols KJ, Palestro CJ. In vitro human leukocyte labeling with 64Cu: An intraindividual comparison with 111In-oxine and 18F-FDG. Nuclear Medicine and Biology. 2009;**36**:545-549

[16] Niccoli Asabella A, Cascini GL, Altini C, Paparella D, Notaristefano A, Rubini G. The copper radioisotopes: A systematic review with special interest to 64Cu. BioMed Research International. 7 May 2014;**2014**:786463. DOI: 10.1155/2014/786463

[17] Lewis JS, Herrero P, Sharp TL, Engelbach JA, Fujibayashi Y, Laforest R, et al. Delineation of hypoxia in canine myocardium using PET and copper (II)-diacetyl-bis(N4-methylthiosemicarbazone). Journal of Nuclear Medicine. 2002;**43**:1557-1569

[18] Holland JP, Ferdani R, Anderson CJ, Lewis JS. Copper-64 radiopharmaceuticals for oncologic imaging. PET Clinics. 2009;**4**:49-67

[19] Jauregui-Osoro M, De Robertis S, Halsted P, Gould S-M, Yu Z, Paul RL, et al. Production of copper-64 using a hospital cyclotron: Targetry, purification and quality analysis. Nuclear Medicine Communications. 2021;**42**:1024

[20] Jødal L, Le Loirec C, Champion C. Positron range in PET imaging: Non-conventional isotopes. Physics in Medicine & Biology. 2014;**59**:7419

[21] Palmer MR, Zhu X, Parker JA. Modeling and simulation of positron range effects for high resolution PET imaging. IEEE Transactions on Nuclear Science. 2005;**52**:1391-1395

[22] Dearling JL, Lewis JS, Mullen GE, Welch MJ, Blower PJ. Copper bis (thiosemicarbazone) complexes as hypoxia imaging agents: Structure-activity relationships. JBIC Journal of Biological Inorganic Chemistry. 2002;**7**:249-259

[23] Handley MG, Medina RA, Mariotti E, Kenny GD, Shaw KP, Yan R, et al. Cardiac hypoxia imaging: Second-generation analogues of 64Cu-ATSM. Journal of Nuclear Medicine. 2014;**55**:488-494

[24] Fleming IN, Manavaki R, Blower PJ, West C, Williams KJ, Harris AL, et al. Imaging tumour hypoxia with positron emission tomography. British Journal of Cancer. 2015;**112**:238-250

[25] Wallhaus TR, Lacy J, Stewart R, Bianco J, Green MA, Nayak N, et al. Copper-62-pyruvaldehyde bis (N4-methyl-thiosemicarbazone) PET imaging in the detection of coronary artery disease in humans. Journal of Nuclear Cardiology. 2001;**8**:67-74

[26] Peng F, Lutsenko S, Sun X, Muzik O. Imaging copper metabolism imbalance in Atp7b−/− knockout mouse model of Wilson's disease with PET-CT and orally administered 64 CuCl 2. Molecular Imaging and Biology. 2012;**14**:600-607

[27] Andreozzi EM, Torres JB, Sunassee K, Dunn J, Walker-Samuel S, Szanda I, et al. Studies of copper trafficking in a mouse model of Alzheimer's disease by positron emission tomography: Comparison of 64Cu acetate and 64CuGTSM. Metallomics. 2017;**9**:1622-1633

[28] Bartnicka JJ, Blower PJ. Insights into trace metal metabolism in health and disease from PET:"PET Metallomics". Journal of Nuclear Medicine. 2018;**59**:1355-1359

[29] Torres JB, Andreozzi EM, Dunn JT, Siddique M, Szanda I, Howlett DR, et al. PET imaging of copper trafficking in a mouse model of Alzheimer disease. Journal of Nuclear Medicine. 2016;**57**:109-114

[30] Griessinger CM, Kehlbach R, Bukala D, Wiehr S, Bantleon R, Cay F, et al. In vivo tracking of Th1 cells by

PET reveals quantitative and temporal distribution and specific homing in lymphatic tissue. Journal of Nuclear Medicine. 2014;**55**:301-307

[31] Nomura S, Nozaki S, Hamazaki T, Takeda T, Ninomiya E, Kudo S, et al. PET imaging analysis with 64Cu in disulfiram treatment for aberrant copper biodistribution in Menkes disease mouse model. Journal of Nuclear Medicine. 2014;**55**:845-851

[32] Fodero-Tavoletti MT, Villemagne VL, Paterson BM, White AR, Li Q-X, Camakaris J, et al. Bis (thiosemicarbazonato) Cu-64 complexes for positron emission tomography imaging of Alzheimer's disease. Journal of Alzheimer's Disease. 2010;**20**:49-55

[33] Hickey JL, Lim S, Hayne DJ, Paterson BM, White JM, Villemagne VL, et al. Diagnostic imaging agents for Alzheimer's disease: Copper radiopharmaceuticals that target Aβ plaques. Journal of the American Chemical Society. 2013;**135**:16120-16132

[34] Piccardo A, Paparo F, Puntoni M, Righi S, Bottoni G, Bacigalupo L, et al. 64CuCl2 PET/CT in prostate cancer relapse. Journal of Nuclear Medicine. 2018;**59**:444-451

[35] Ferrari C, Niccoli Asabella A, Villano C, Giacobbi B, Coccetti D, Panichelli P, et al. Copper-64 dichloride as theranostic agent for glioblastoma multiforme: A preclinical study. BioMed Research International. Hindawi Publishing Corporation. 2015;**2015**:6. Article ID 129764. DOI: 10.1155/2015/129764

[36] Jing X, Yang F, Shao C, Wei K, Xie M, Shen H, et al. Role of hypoxia in cancer therapy by regulating the tumor microenvironment. Molecular Cancer. 2019;**18**:1-15

[37] Sørensen BS, Horsman MR. Tumor hypoxia: Impact on radiation therapy and molecular pathways. Frontiers in Oncology. 2020;**10**:562

[38] Wong R, Fyles A, Milosevic M, Pintilie M, Hill RP. Heterogeneity of polarographic oxygen tension measurements in cervix cancer: An evaluation of within and between tumor variability, probe position, and track depth. International Journal of Radiation Oncology, Biology, Physics. 1997;**39**:405-412

[39] Lyng H, Malinen E. Hypoxia in cervical cancer: From biology to imaging. Clinical and Translational Imaging. 2017;**5**:373-388

[40] Matsumoto K-I, Szajek L, Krishna MC, Cook JA, Seidel J, Grimes K, et al. The influence of tumor oxygenation on hypoxia imaging in murine squamous cell carcinoma using [64Cu] Cu-ATSM or [18F] Fluoromisonidazole positron emission tomography. International Journal of Oncology. 2007;**30**:873-881

[41] Nie X, Elvington A, Laforest R, Zheng J, Voller TF, Zayed MA, et al. 64Cu-ATSM positron emission tomography/magnetic resonance imaging of hypoxia in human atherosclerosis. Circulation: Cardiovascular Imaging. 2020;**13**:e009791

[42] Liu J, Hajibeigi A, Ren G, Lin M, Siyambalapitiyage W, Liu Z, et al. Retention of the radiotracers 64Cu-ATSM and 64Cu-PTSM in human and murine tumors is influenced by MDR1 protein expression. Journal of Nuclear Medicine. 2009;**50**:1332-1339

[43] Fujibayashi Y, Taniuchi H, Yonekura Y, Ohtani H. Copper-62-ATSM: A new hypoxia imaging agent with high membrane permeability and low

redox potential. The Journal of Nuclear Medicine. 1997;**38**:1155

[44] Fujibayashi Y, Cutler C, Anderson C, McCarthy D, Jones L, Sharp T, et al. Comparative studies of Cu-64-ATSM and C-11-acetate in an acute myocardial infarction model: Ex vivo imaging of hypoxia in rats. Nuclear Medicine and Biology. 1999;**26**:117-121

[45] Dearling JL, Blower PJ. Redox-active metal complexes for imaging hypoxic tissues: Structure–activity relationships in copper (II) bis (thiosemicarbazone) complexes. Chemical Communications. 1998;(22):2531-2532. DOI: 10.1039/a805957h

[46] Tanaka T, Furukawa T, Fujieda S, Kasamatsu S, Yonekura Y, Fujibayashi Y. Double-tracer autoradiography with Cu-ATSM/FDG and immuno-histochemical interpretation in four different mouse implanted tumor models. Nuclear Medicine and Biology. 2006;**33**:743-750

[47] Yuan H, Schroeder T, Bowsher JE, Hedlund LW, Wong T, Dewhirst MW. Intertumoral differences in hypoxia selectivity of the PET imaging agent 64Cu (II)-diacetyl-bis (N4-methylthiosemicarbazone). Journal of Nuclear Medicine. 2006;**47**:989-998

[48] Dence CS, Ponde DE, Welch MJ, Lewis JS. Autoradiographic and small-animal PET comparisons between 18F-FMISO, 18F-FDG, 18F-FLT and the hypoxic selective 64Cu-ATSM in a rodent model of cancer. Nuclear Medicine and Biology. 2008;**35**:713-720

[49] Holland JP, Barnard PJ, Collison D, Dilworth JR, Edge R, Green JC, et al. Spectroelectrochemical and computational studies on the mechanism of hypoxia selectivity of copper radiopharmaceuticals. Chemistry–A European Journal. 2008;**14**:5890-5907

[50] Liu T, Karlsen M, Karlberg AM, Redalen KR. Hypoxia imaging and theranostic potential of [64 Cu] [Cu (ATSM)] and ionic Cu (II) salts: A review of current evidence and discussion of the retention mechanisms. EJNMMI Research. 2020;**10**:1-14

[51] Lewis JS, McCarthy DW, McCarthy TJ, Fujibayashi Y, Welch MJ. Evaluation of 64Cu-ATSM in vitro and in vivo in a hypoxic tumor model. Journal of Nuclear Medicine. 1999;**40**:177-183

[52] Lapi SE, Lewis JS, Dehdashti F. Evaluation of hypoxia with copper-labeled diacetyl-bis (N-methylthiosemicarbazone). In: Seminars in Nuclear Medicine. Elsevier; 2015. pp. 177-185

[53] Colombié M, Gouard S, Frindel M, Vidal A, Chérel M, Kraeber-Bodéré F, et al. Focus on the controversial aspects of 64Cu-ATSM in tumoral hypoxia mapping by PET imaging. Frontiers in Medicine. 2015;**2**:58

[54] Lewis JS, Laforest R, Dehdashti F, Grigsby PW, Welch MJ, Siegel BA. An imaging comparison of 64Cu-ATSM and 60Cu-ATSM in cancer of the uterine cervix. Journal of Nuclear Medicine. 2008;**49**:1177-1182

[55] Anderson CJ, Ferdani R. Copper-64 radiopharmaceuticals for PET imaging of cancer: Advances in preclinical and clinical research. Cancer Biotherapy and Radiopharmaceuticals. 2009;**24**:379-393

[56] Gangemi V, Mignogna C, Guzzi G, Lavano A, Bongarzone S, Cascini GL, et al. Impact of [64 Cu][Cu (ATSM)] PET/CT in the evaluation of hypoxia in a patient with glioblastoma: A case report. BMC Cancer. 2019;**19**:1-4

[57] Bourgeois M, Rajerison H, Guerard F, Mougin-Degraef M, Barbet J, Michel N, et al. Contribution of [64Cu]-ATSM PET

in molecular imaging of tumour hypoxia compared to classical [18F]-MISO—A selected review. Nuclear Medicine Review. 2011;**14**:90-95

[58] Dehdashti F, Mintun MA, Lewis JS, Bradley J, Govindan R, Laforest R, et al. In vivo assessment of tumor hypoxia in lung cancer with 60 Cu-ATSM. European Journal of Nuclear Medicine and Molecular Imaging. 2003;**30**:844-850

[59] Lopci E, Grizzi F, Russo C, Toschi L, Grassi I, Cicoria G, et al. Early and delayed evaluation of solid tumours with 64Cu-ATSM PET/CT: A pilot study on semiquantitative and computer-aided fractal geometry analysis. Nuclear Medicine Communications. 2017;**38**:340-346

[60] Grassi I, Nanni C, Cicoria G, Blasi C, Bunkheila F, Lopci E, et al. Usefulness of 64Cu-ATSM in head and neck cancer: A preliminary prospective study. Clinical Nuclear Medicine. 2014;**39**:e59-e63

[61] Vahidfar N, Farzanefar S, Ahmadzadehfar H, Molloy EN, Eppard E. A review of nuclear medicine approaches in the diagnosis and the treatment of gynecological malignancies. Cancers. 2022;**14**:1779

[62] Hueting R. Radiocopper for the imaging of copper metabolism. Journal of Labelled Compounds and Radiopharmaceuticals. 2014;**57**:231-238

[63] Mortimer JE, Kruper L, Cianfrocca M, Lavasani S, Liu S, Tank-Patel N, et al. Use of HER2-directed therapy in metastatic breast cancer and how community physicians collaborate to improve care. Journal of Clinical Medicine. 2020;**9**:1984

[64] Arienti C, Pignatta S, Tesei A. Epidermal growth factor receptor family and its role in gastric cancer. Frontiers in Oncology. 2019;**9**:1308

[65] Hayes DF. HER2 and breast cancer—A phenomenal success story. New England Journal of Medicine. 2019;**381**:1284-1286

[66] Slamon DJ, Clark GM, Wong SG, Levin WJ, Ullrich A, McGuire WL. Human breast cancer: Correlation of relapse and survival with amplification of the HER-2/neu oncogene. Science. 1987;**235**:177-182

[67] Press MF, Pike MC, Chazin VR, Hung G, Udove JA, Markowicz M, et al. Her-2/neu expression in node-negative breast cancer: Direct tissue quantitation by computerized image analysis and association of overexpression with increased risk of recurrent disease. Cancer Research. 1993;**53**:4960-4970

[68] Giordano SH, Temin S, Chandarlapaty S, Crews JR, Esteva FJ, Kirshner JJ, et al. Systemic therapy for patients with advanced human epidermal growth factor receptor 2–positive breast cancer: ASCO clinical practice guideline update. Journal of Clinical Oncology. 2018;**36**:2736-2740

[69] Jarrett AM, Hormuth DA, Adhikarla V, Sahoo P, Abler D, Tumyan L, et al. Towards integration of 64Cu-DOTA-trastuzumab PET-CT and MRI with mathematical modeling to predict response to neoadjuvant therapy in HER2+ breast cancer. Scientific Reports. 2020;**10**:1-14

[70] Kurihara H, Hamada A, Yoshida M, Shimma S, Hashimoto J, Yonemori K, et al. 64Cu-DOTA-trastuzumab PET imaging and HER2 specificity of brain metastases in HER2-positive breast cancer patients. EJNMMI Research. 2015;**5**:1-8

[71] Tamura K, Kurihara H, Yonemori K, Tsuda H, Suzuki J, Kono Y, et al. 64Cu-DOTA-trastuzumab PET imaging in patients with HER2-positive

breast cancer. Journal of Nuclear Medicine. 2013;**54**:1869-1875

[72] Bang Y-J, Van Cutsem E, Feyereislova A, Chung HC, Shen L, Sawaki A, et al. Trastuzumab in combination with chemotherapy versus chemotherapy alone for treatment of HER2-positive advanced gastric or gastro-oesophageal junction cancer (ToGA): A phase 3, open-label, randomised controlled trial. The Lancet. 2010;**376**:687-697

[73] Guo X, Zhu H, Zhou N, Chen Z, Liu T, Liu F, et al. Noninvasive detection of HER2 expression in gastric cancer by 64Cu-NOTA-trastuzumab in PDX mouse model and in patients. Molecular Pharmaceutics. 2018;**15**:5174-5182

[74] Chopra A. 64Cu-labeled DOTA-conjugated rituximab, a chimeric murine/human anti-CD20 monoclonal antibody. In: Molecular Imaging and Contrast Agent Database (MICAD) [Internet]. NLM, Bethesda: National Center for Biotechnology Information; 2012

[75] Natarajan A, Arksey N, Iagaru A, Chin FT, Gambhir SS. Validation of 64Cu-DOTA-rituximab injection preparation under good manufacturing practices: A PET tracer for imaging of B-cell non-Hodgkin lymphoma. Molecular Imaging. 2015;**14**. DOI: 10.2310/7290.2014.00055. PMID: 25762106

[76] Natarajan A, Gowrishankar G, Nielsen CH, Wang S, Iagaru A, Goris ML, et al. Positron emission tomography of 64Cu-DOTA-Rituximab in a transgenic mouse model expressing human CD20 for clinical translation to image NHL. Molecular Imaging and Biology. 2012;**14**:608-616

[77] James ML, Hoehne A, Mayer AT, Lechtenberg K, Moreno M, Gowrishankar G, et al. Imaging B cells in a mouse model of multiple sclerosis using 64Cu-rituximab PET. Journal of Nuclear Medicine. 2017;**58**:1845-1851

[78] Johnbeck CB, Knigge U, Loft A, Berthelsen AK, Mortensen J, Oturai P, et al. Head-to-head comparison of 64Cu-DOTATATE and 68Ga-DOTATOC PET/CT: A prospective study of 59 patients with neuroendocrine tumors. Journal of Nuclear Medicine. 2017;**58**:451-457

[79] Malmberg C, Ripa RS, Johnbeck CB, Knigge U, Langer SW, Mortensen J, et al. 64Cu-DOTATATE for noninvasive assessment of atherosclerosis in large arteries and its correlation with risk factors: Head-to-head comparison with 68Ga-DOTATOC in 60 patients. Journal of Nuclear Medicine. 2015;**56**:1895-1900

[80] Delpassand ES, Ranganathan D, Wagh N, Shafie A, Gaber A, Abbasi A, et al. 64Cu-DOTATATE PET/CT for imaging patients with known or suspected somatostatin receptor–positive neuroendocrine tumors: Results of the first US prospective, reader-masked clinical trial. Journal of Nuclear Medicine. 2020;**61**:890-896

[81] Carlsen EA, Johnbeck CB, Binderup T, Loft M, Pfeifer A, Mortensen J, et al. 64Cu-DOTATATE PET/CT and prediction of overall and progression-free survival in patients with neuroendocrine neoplasms. Journal of Nuclear Medicine. 2020;**61**:1491-1497

[82] de Camargo Etchebehere ECS, de Oliveira SA, Gumz B, Vicente A, Hoff PG, Corradi G, et al. 68Ga-DOTATATE PET/CT, 99mTc-HYNIC-octreotide SPECT/CT, and whole-body MR imaging in detection of neuroendocrine tumors: A prospective trial. Journal of Nuclear Medicine. 2014;**55**:1598-1604

[83] Bodei L, Ambrosini V, Herrmann K, Modlin I. Current concepts in

68Ga-DOTATATE imaging of neuroendocrine neoplasms: Interpretation, biodistribution, dosimetry, and molecular strategies. Journal of Nuclear Medicine. 2017;**58**:1718-1726

[84] Pfeifer A, Knigge U, Binderup T, Mortensen J, Oturai P, Loft A, et al. 64Cu-DOTATATE PET for neuroendocrine tumors: A prospective head-to-head comparison with 111In-DTPA-octreotide in 112 patients. Journal of Nuclear Medicine. 2015;**56**:847-854

[85] Hicks RJ, Jackson P, Kong G, Ware RE, Hofman MS, Pattison DA, et al. 64Cu-SARTATE PET imaging of patients with neuroendocrine tumors demonstrates high tumor uptake and retention, potentially allowing prospective dosimetry for peptide receptor radionuclide therapy. Journal of Nuclear Medicine. 2019;**60**:777-785

[86] Johnbeck CB, Knigge U, Kjær A. PET tracers for somatostatin receptor imaging of neuroendocrine tumors: Current status and review of the literature. Future Oncology. 2014;**10**:2259-2277

[87] Mirzaei S, Revheim M-E, Raynor W, Zehetner W, Knoll P, Zandieh S, et al. 64Cu-DOTATOC PET-CT in patients with neuroendocrine tumors. Oncology and Therapy. 2020;**8**:125-131

[88] Vahidfar N, Fallahpoor M, Farzanehfar S, Divband G, Ahmadzadehfar H. Historical review of pharmacological development and dosimetry of PSMA-based theranostics for prostate cancer. Journal of Radioanalytical and Nuclear Chemistry. 2019;**322**:237-248

[89] Calabria F, Pichler R, Leporace M, Wolfsgruber J, Coscarelli P, Dunzinger A, et al. 68Ga/64Cu PSMA bio-distribution in prostate cancer patients: Potential pitfalls for different tracers. Current Radiopharmaceuticals. 2019;**12**:238-246

[90] Vali R, Loidl W, Pirich C, Langesteger W, Beheshti M. Imaging of prostate cancer with PET/CT using 18F-Fluorocholine. American Journal of Nuclear Medicine and Molecular Imaging. 2015;**5**:96

[91] Morris MJ, Akhurst T, Osman I, Nunez R, Macapinlac H, Siedlecki K, et al. Fluorinated deoxyglucose positron emission tomography imaging in progressive metastatic prostate cancer. Urology. 2002;**59**:913-918

[92] Sanz G, Robles J, Gimenez M, Arocena J, Sanchez D, Rodriguez-Rubio F, et al. Positron emission tomography with 18fluorine-labelled deoxyglucose: Utility in localized and advanced prostate cancer. BJU International. 1999;**84**:1028-1031

[93] Minamimoto R, Uemura H, Sano F, Terao H, Nagashima Y, Yamanaka S, et al. The potential of FDG-PET/CT for detecting prostate cancer in patients with an elevated serum PSA level. Annals of Nuclear Medicine. 2011;**25**:21-27

[94] Effert P, Beniers A, Tamimi Y, Handt S, Jakse G. Expression of glucose transporter 1 (Glut-1) in cell lines and clinical specimens from human prostate adenocarcinoma. Anticancer Research. 2004;**24**:3057-3064

[95] Shiiba M, Ishihara K, Kimura G, Kuwako T, Yoshihara N, Sato H, et al. Evaluation of primary prostate cancer using 11C-methionine-PET/CT and 18F-FDG-PET/CT. Annals of Nuclear Medicine. 2012;**26**:138-145

[96] Kennedy EP, Weiss SB. The function of cytidine coenzymes in the biosynthesis of phospholipides. Journal of Biological Chemistry. 1956;**222**:193-214

[97] Wang Y, Kent C. Effects of altered phosphorylation sites on the properties of CTP: Phosphocholine cytidylyltransferase. Journal of Biological Chemistry. 1995;**270**:17843-17849

[98] Beheshti M, Imamovic L, Broinger G, Vali R, Waldenberger P, Stoiber F, et al. 18F choline PET/CT in the preoperative staging of prostate cancer in patients with intermediate or high risk of extracapsular disease: A prospective study of 130 patients. Radiology. 2010;**254**:925-933

[99] Chondrogiannis S, Marzola MC, Grassetto G, Maffione AM, Rampin L, Veronese E, et al. New acquisition protocol of 18F-choline PET/CT in prostate cancer patients: Review of the literature about methodology and proposal of standardization. BioMed Research International. 2014;**2014**. DOI: 10.1155/2014/215650. PMID: 25121090; PMCID: PMC4119889

[100] Hodolic M. Role of 18F-choline PET/CT in evaluation of patients with prostate carcinoma. Radiology and Oncology. 2011;**45**:17

[101] Cantiello F, Crocerossa F, Russo GI, Gangemi V, Ferro M, Vartolomei MD, et al. Comparison between 64Cu-PSMA-617 PET/CT and 18F-choline PET/CT imaging in early diagnosis of prostate cancer biochemical recurrence. Clinical Genitourinary Cancer. 2018;**16**:385-391

[102] Grubmüller B, Baum RP, Capasso E, Singh A, Ahmadi Y, Knoll P, et al. 64Cu-PSMA-617 PET/CT imaging of prostate adenocarcinoma: First in-human studies. Cancer Biotherapy and Radiopharmaceuticals. 2016;**31**:277-286

[103] Capasso E, Durzu S, Piras S, Zandieh S, Knoll P, Haug A, et al. Role of 64CuCl2 PET/CT in staging of prostate cancer. Annals of Nuclear Medicine. 2015;**29**:482-488

[104] Sparks R, Peng F. Positron emission tomography of altered copper metabolism for metabolic imaging and personalized therapy of prostate cancer. Journal of Radiology and Radiation Therapy. 2013;**1**:1015

[105] Hoberück S, Wunderlich G, Michler E, Hölscher T, Walther M, Seppelt D, et al. Dual-time-point 64 Cu-PSMA-617-PET/CT in patients suffering from prostate cancer. Journal of Labelled Compounds and Radiopharmaceuticals. 2019;**62**:523-532

[106] Cantiello F, Gangemi V, Cascini GL, Calabria F, Moschini M, Ferro M, et al. Diagnostic accuracy of 64copper prostate-specific membrane antigen positron emission tomography/ computed tomography for primary lymph node staging of intermediate-to high-risk prostate cancer: Our preliminary experience. Urology. 2017;**106**:139-145

[107] Woo S-K, Jang SJ, Seo M-J, Park JH, Kim BS, Kim EJ, et al. Development of 64Cu-NOTA-trastuzumab for HER2 targeting: A radiopharmaceutical with improved pharmacokinetics for human studies. Journal of Nuclear Medicine. 2019;**60**:26-33

[108] Liu T, Liu C, Zhang Z, Zhang N, Guo X, Xia L, et al. 64Cu-PSMA-BCH: A new radiotracer for delayed PET imaging of prostate cancer. European Journal of Nuclear Medicine and Molecular Imaging. 2021;**48**:4508-4516

[109] Pfeifer A, Knigge U, Mortensen J, Oturai P, Berthelsen AK, Loft A, et al. Clinical PET of neuroendocrine tumors using 64Cu-DOTATATE: First-in-humans study. Journal of Nuclear Medicine. 2012;**53**:1207-1215

[110] Matias M, Pinho JO, Penetra MJ, Campos G, Reis CP, Gaspar MM. The

challenging melanoma landscape: From early drug discovery to clinical approval. Cell. 2021;**10**:3088

[111] Anderson CJ, Dehdashti F, Cutler PD, Schwarz SW, Laforest R, Bass LA, et al. 64Cu-TETA-octreotide as a PET imaging agent for patients with neuroendocrine tumors. Journal of Nuclear Medicine. 2001;**42**:213-221

[112] Persson M, Skovgaard D, Brandt-Larsen M, Christensen C, Madsen J, Nielsen CH, et al. First-in-human uPAR PET: Imaging of cancer aggressiveness. Theranostics. 2015;**5**:1303

[113] Ahrens BJ, Li L, Ciminera AK, Chea J, Poku E, Bading JR, et al. Diagnostic PET imaging of mammary microcalcifications using 64Cu-DOTA-alendronate in a rat model of breast cancer. Journal of Nuclear Medicine. 2017;**58**:1373-1379

[114] Avila-Rodriguez M, Rios C, Carrasco-Hernandez J, Manrique-Arias J, Martinez-Hernandez R, Garcia-Perez F, et al. Biodistribution and radiation dosimetry of [64Cu] copper dichloride: First-in-human study in healthy volunteers. EJNMMI Research. 2017;**7**:1-7

[115] Laforest R, Dehdashti F, Lewis JS, Schwarz SW. Dosimetry of 60/61/62/64Cu-ATSM: A hypoxia imaging agent for PET. European Journal of Nuclear Medicine and Molecular Imaging. 2005;**32**:764-770